Nannofossil imprints across the Paleocene-Eocene Thermal Maximum

Sam M. Slater[1*], Paul R. Bown[2] and Phillip E. Jardine[3]

[1]Department of Palaeobiology, Swedish Museum of Natural History, Stockholm, SE-104 05, Sweden.

[2]Department of Earth Sciences, University College London, London, WC1E 6BT, UK.

[3]Institute of Geology and Palaeontology, University of Münster, Münster, D-48149, Germany.

*sam.slater@nrm.se

ABSTRACT

The Paleocene-Eocene Thermal Maximum (PETM; ~56 million years ago) geological interval records a marked decline in calcium carbonate ($CaCO_3$) in seafloor sediments, potentially reflecting an episode of deep- and possibly shallow-water ocean acidification. However, because $CaCO_3$ is susceptible to post-burial dissolution, it remains uncertain to what extent this process has influenced the PETM geological record. Here we test for evidence of post-burial dissolution by searching for imprint fossils of nannoplankton preserved on organic matter. We studied a PETM succession from the South Dover Bridge (SDB) core, Maryland, USA, comparing our imprint record with previously published data from traditionally sampled $CaCO_3$-preserved nannoplankton body fossils. Abundant imprints through intervals devoid of $CaCO_3$ would signify that post-burial dissolution removed much of the $CaCO_3$ from the rock record. Imprints were recorded from most samples but were rare and of low diversity. Body fossils are substantially more numerous and diverse, capturing a more complete record of the living nannoplankton communities through the PETM. The SDB succession records a dissolution zone/low carbonate interval at the onset of the PETM, through which nannoplankton body fossils are rare. No nannoplankton imprints were found from this interval, suggesting that the rarity of body fossils is unlikely to have been the result of post-buria dissolution. Instead, our findings suggest that declines in $CaCO_3$ through the PETM of SDB were the result of: (i) biotic responses to changes that were happening during this event, and/or (ii) $CaCO_3$ dissolution that occurred before lithification (i.e., in the water column or at the seafloor).

INTRODUCTION

The Paleocene–Eocene Thermal Maximum (PETM; ~56 million years ago) was a geologically rapid global warming event, lasting ~200 thousand years, throughout which global temperatures increased by ~5–8 °C (McInerney & Wing 2011 and references therein). The event was likely caused by a massive injection of isotopically light carbon into the ocean–atmosphere system over several thousands of years (McInerney & Wing 2011; Turner 2018), although the carbon sources and ultimate trigger of the PETM are still debated (e.g., McInerney & Wing 2011; Kender et al., 2021). In the geological record, marine PETM successions are generally characterized by major declines in calcium carbonate ($CaCO_3$) (Zachos et al., 2005) alongside marked changes in micro- and nanno-fossil assemblages, including benthic foraminiferal extinctions (Thomas 1989, 2003, 2007), calcareous nannoplankton species turnover (Gibbs et al., 2006) and reduced nannoplankton calcification rates (O'Dea et al., 2014). Together with boron-based proxy evidence (Penman et al., 2014; Babila et al., 2018, 2022), such signals are commonly associated with deep-, and possibly shallow-water, ocean acidification (OA) (Zachos et al., 2005; Kump et al., 2009; Gibbs et al., 2010; Bralower et al., 2018; Babila et al., 2022), and/or other environmental changes, such as elevated sea surface temperatures (Aze et al., 2014). However, the extent to which post-burial $CaCO_3$ dissolution – also termed chemical erosion (Bralower et al., 2014) – has affected these records is difficult to determine, and where severe dissolution has likely taken place, its timing generally remains unclear.

Imprint fossils of nannoplankton preserved on organic matter provide a tool to test the degree and timing of $CaCO_3$ dissolution throughout intervals where $CaCO_3$ preservation is poor (Slater et al., 2022). Although other approaches have been applied to PETM strata to understand the impact of dissolution, such as foraminiferal fragmentation and dissolution of nannofossil rims and central areas (Bralower et al., 2014), these methods rely on the preservation of $CaCO_3$ and are not necessarily indicative of the timing of dissolution. For example, dissolution of nannofossil liths could occur at any point after their formation; in the water column, at the seafloor, or after deposition and lithification. Nannofossil imprints, however, can be preserved in sediments devoid of $CaCO_3$, and where this is the case, they can reveal that $CaCO_3$ has been removed from the rock record after deposition (Slater et al., 2022).

Here we searched for nannofossil imprints through a PETM succession from the South Dover Bridge (SDB) core, southern Maryland, USA [38°44′49.34″N, 76°00′25.09″W] (Fig. 1; drilled by the U.S. Geological Survey), with the aim to determine the timing of potential $CaCO_3$ dissolution. The SDB section was chosen because it represents a relatively shallow water marine environment (~120–150 meters depth) (Self-Trail et al., 2012; Robinson and Spivey 2019) that preserves organic matter

(Alemán González et al., 2012; Edwards 2012), required for imprint preservation (Batten 1985; Slater et al., 2022). Furthermore, the succession appears to record a spectrum of dissolution conditions through the PETM interval, from little to no dissolution below and above the CIE, to pervasive dissolution at the base of the carbon isotope excursion (CIE). The calcareous nannoplankton 'body' fossils (i.e., the calcite fossil remains of nannoplankton cell wall coverings) from this succession have previously been studied in detail, with diverse and abundant assemblages spanning the PETM described by Self-Trail (2011), Alemán González et al. (2012) and Self-Trail et al., (2012). A notable ~2-m-thick dissolution zone has been recognized near the base of the CIE, through which nannoplankton body fossils are extremely sparse (Self-Trail 2011; Self-Trail et al., 2012). Bralower et al. (2018) described a low carbonate interval (LCI) – representing a slightly amended version of the dissolution zone – from several PETM sections across Maryland and New Jersey, including the SDB core. Bralower et al. (2018) discussed numerous possible causes for the LCI, hypothesizing that this was likely due to shoaling of the lysocline and calcite compensation depth (CCD), but that eutrophication and microbial activity potentially exacerbated the impact of acidification. Further proxy-based reconstructions of seawater pH from the SDB core have inferred that OA started prior to the main CIE, during a pre-onset excursion (Babila et al., 2022). Indeed, these studies point to relatively shallow-water OA. However, rich and abundant nannofossil imprints preserved within the sediments low in $CaCO_3$ could reveal that $CaCO_3$ was removed by diagenetic dissolution, rather than *in situ* water column OA or changes to the CCD or lysocline depth that affected seafloor carbonate. Such results would not necessarily discount that changes to seawater chemistry influenced $CaCO_3$ PETM records, but could provide an indication of the extent of diagenetic $CaCO_3$ dissolution.

Post-drilling dissolution of carbonate is common in organic-rich sediments of the Atlantic Coastal Plain, likely due to pyrite oxidation, thus sampling for body fossils needs to occur as soon as possible after coring (Self-Trail & Seefelt 2005; Self-Trail 2011). This is likely why the sediments of the Marlboro Clay in the SDB core record abundant body fossils, whereas their outcrop counterparts are generally barren or yield very sparse nannofossils (Bybell & Gibson 1991; Bybell & Gibson 1994; Gibson & Bybell 1994; Self-Trail 2011). As the SDB core was recovered in 2007, it is probable that at least some post-drilling dissolution of $CaCO_3$ has taken place; a secondary goal of this study was therefore to examine the nannofossil assemblages using an approach that may be immune to the modifying effects of diagenetic and post-drilling dissolution, by studying their imprints.

METHODS

We examined 12 samples spanning the PETM of SDB (Fig. 2). Rock samples were dissolved in HCl and HF and resultant residues were sieved at 5 µm to isolate organic matter. Processing was conducted at Global Geolab Limited, Canada. Final residues were studied using light microscopy (LM) with an Olympus BX53 and scanning electron microscopy (SEM) using an ESEM FEI Quanta FEG 650 scanning electron microscope at the Swedish Museum of Natural History.

For LM, residues were strewn across cover slips and mounted onto glass slides with epoxy resin. To assess the composition of organic matter, palynofacies analysis was conducted, where a minimum of 300 organic particles were counted per sample (see Table S1 for palynofacies categories).

For SEM, residues were strewn across SEM stubs, dried and gold coated. Organic matter on SEM stubs was observed in systematic traverses for 2 hours per sample at ×10,000 magnification, followed by 30 minutes at ×5,000 magnification, through which all potential imprints were photographed; followed by 30 minutes at ×5,000 magnification to search for well-preserved specimens. Unprocessed rock material from two samples (PJ-SDB13-003 and PJ-SDB13-004) was also examined for imprints and body fossils. For this approach, freshly cleaved rock was mounted onto SEM stubs, gold coated and examined for 2 hours per sample at ×10,000 magnification.

RESULTS

Nannofossil Imprints

We found imprints in nine of the 12 investigated samples (Fig. 2; Table S1). Including indeterminate coccoliths, eight taxa were recorded (Fig. 2). Preservation was variable, with a mixture of well-preserved (Fig. 2B, C) and poorly preserved (Fig. 2G) specimens.

Nannofossil Imprints vs. Body Fossils

Imprint assemblages were considerably less rich than previously sampled body fossils, demonstrating that body fossils capture a more complete record of nannoplankton through the PETM of SDB (Fig. 3). Previous studies have shown that body fossils are extremely sparse through the dissolution zone/LCI (Fig. 3; Self-Trail 2011; Self-Trail et al., 2012; Bralower et al., 2018). Observations of rock surfaces and organic residues from the sample taken from the dissolution zone/LCI here (PJ-SDB13-003), reveal similar findings; one taxon, either *Braarudosphaera* sp. or *Micrantholithus* sp. (a more definitive identification was difficult since only a side-view was visible), was recorded on rock surfaces (Figure S1), and no imprints were found in organic residues. For sample PJ-SDB13-004, which yielded the richest imprint assemblage, body fossils on rock surfaces were common and well-preserved (Figure S1).

Organic Matter

Palynofacies assemblages were co-dominated by phytoclasts, amorphous organic matter (AOM) and marine palynomorphs. The dinoflagellate, *Apectodinium*, was present through the PETM, recording the acme interval associated with this event (Bujak and Brinkhuis 1998; Crouch et al., 2001). Amorphous organic matter increases in relative abundance around the onset of the CIE, within the dissolution zone/LCI, reflecting a relative increase in organic matter deposition, and a corresponding decline in $CaCO_3$ preservation, associated with the PETM (Zachos et al., 2005; Schneider-Mor & Bowen 2013).

DISCUSSION

The rarity of nannofossil imprints across the PETM suggests that the taphonomic conditions required for their preservation were sub-optimal compared to body fossils (Fig. 3; Self-Trail 2011; Self-Trail et al., 2012). Imprints were only recorded from strata that also yielded body fossils (Fig. 3) and none were found on unprocessed rock surfaces. Hence, rather than representing ‘ghost’ nannofossils – imprints found in rocks that are barren of body fossils (Slater et al., 2022) – imprints here are likely the molds of body fossils that were dissolved during acid digestion in the laboratory.

Although only one sample was examined from the dissolution zone/LCI here, both the absence of imprints and rarity of body fossils suggests that: (i) nannoplankton production declined through the early stages of the PETM; and/or (ii) dissolution of $CaCO_3$ occurred before lithification, in the water column, at the seafloor, or during the earliest stages of diagenesis. If dissolution occurred after lithification, we would expect to find imprints, as overburden would have likely facilitated their formation. At this stage, our data alone cannot discount interpretations (i) or (ii), but previously studied nannoplankton counts with taxon-specific Sr/Ca data from other localities support the hypothesis that the decrease in $CaCO_3$ through the PETM was primarily driven by an increase in seafloor dissolution, rather than a decrease in production in surface waters (Gibbs et al., 2010). The scarcity of imprints suggests that the timing of potential $CaCO_3$ dissolution was unlikely to have been post-lithification and our findings therefore support the hypothesis that shelf acidification linked to shoaling of the lysocline and CCD contributed to the decline in $CaCO_3$ preservation at the onset of the PETM in the SDB region (Bralower et al., 2018).

Nannofossil imprint assemblages from Mesozoic oceanic anoxic events (OAEs), and especially the Toarcian-OAE, are generally richer, more numerous and better preserved than those documented here (Slater et al., 2022). In addition to variations in seawater chemistry, these discrepancies likely also relate to the amount and type of organic matter – and in particular the quantity of AOM, since this is a good substrate for imprinting (Slater et al., 2022) – preserved through these different events and localities. Given that organic matter appears necessary for imprinting, the rarity of imprints through the PETM compared to the OAEs is likely a product of the lower relative abundances of AOM and the generally lower total organic carbon values (Bralower et al., 2018) compared to the OAEs (e.g., McArthur et al. 2008). Furthermore, the preservation of AOM as larger fragments through the OAEs (Slater et al., 2022) appears to be important, because imprints are less distinct on the smaller, highly fragmented pieces that are typical of the PETM of SDB. Although imprints are apparently most common on AOM compared to other types of organic matter, they can also preserve on dinoflagellates

(Downie 1956), prasinophyte algae, and pollen (Slater et al., 2022). The lack of imprints on the dinoflagellate *Apectodinium*, which is abundant through the PETM of SDB, suggests that the surface of this cyst was a poor substrate for imprinting.

Comparisons of imprint and body nannofossil records through the Mesozoic OAEs revealed marked differences in abundance and diversity patterns between these fossil records. In numerous OAE samples, imprint assemblages were substantially more diverse than body fossil records, and in many cases, rich imprint records were found in samples barren of body fossils (Slater et al., 2022). This is not the case for the PETM of SDB. Although the sampling resolution of imprints here is lower than body fossil records (Self-Trail 2011; Self-Trail et al., 2012), the pattern of lower imprint richness through the studied succession is consistent. More generally, the abundance of body fossils and the scarcity of imprints throughout most of the PETM of SDB indicates that post-burial $CaCO_3$ dissolution was less pervasive compared to the OAE records. These observations bolster confidence that traditionally-sampled body fossil records (Self-Trail 2011; Self-Trail et al., 2012) have not been extensively modified by post-burial dissolution and thus provide a relatively good representative signal of the buried $CaCO_3$ in the Atlantic Coastal Plain region.

CONCLUSIONS

Imprint fossils of nannoplankton represent a relatively novel tool with which to test the extent and timing of $CaCO_3$ dissolution through geological intervals where $CaCO_3$ preservation is poor. In the case of the PETM, the scarcity of these fossils through intervals of low $CaCO_3$ preservation suggests that any dissolution to have happened took place before lithification, in the water column or at the seafloor, supporting hypotheses of seafloor and/or potentially shallower-water $CaCO_3$ dissolution. Future studies testing for the presence and abundance of nannofossil imprints through the PETM at higher-resolution, and in deep-water successions elsewhere, will potentially shed more light on the timing of dissolution through this important geological interval.

ACKNOWLEDGMENTS

The Swedish Research Council (2019-04524 [SMS], 2023-03330 [SMS]), Formas (2023-00984 [SMS]), the Royal Swedish Academy of Sciences (GS2021-0018 [SMS]), the Palaeontological Association (Sylvester-Bradley award [PEJ]) and the German Research Foundation (443701866 [PEJ]) funded this research. We thank Andreas Karlsson for assistance with SEM photography. We thank Jean Self-Trail, Timothy Bralower and an anonymous reviewer for their helpful reviews. Who were the samples from???

REFERENCES CITED

Alemán González, W.B., Powars, D.S., Seefelt, E.L., Edwards, L.E., Self-Trail, J.M., Durand, C.T., Schultz, A.P., and McLaughlin, P.P. 2012. Preliminary physical stratigraphy, biostratigraphy, and geophysical data of the USGS South Dover Bridge Core, Talbot County, Maryland: U.S. Geological Survey Open-File Report, v. 2012–1218, p. 1–16.

Aze, T., Pearson, P.N., Dickson, A.J., Badger, M.P.S., Bown, P.R., Pancost, R.D., Gibbs, S.J., Huber, B.T., Leng, M.J., Coe, A.L., Cohen, A.S., and Foster, G.L. 2014. Extreme warming of tropical waters during the Paleocene–Eocene Thermal Maximum: Geology, v. 42, p. 739–742, https://doi.org/10.1130/G35637.1.

Babila, T.L., Penman, D.E., Hönisch, B., Kelly, D.C., Bralower, T.J., Rosenthal, Y., and Zachos J.C. 2018. Capturing the global signature of surface ocean acidification during the Palaeocene–Eocene Thermal Maximum: Philosophical Transactions of the Royal Society A, v. 376, article, 20170072, http://dx.doi.org/10.1098/rsta.2017.0072.

Babila, T.L., Penman, D.E., Standish, C.D., Doubrawa, M., Bralower, T.J., Robinson, M.M., Self-Trail, J.M., Speijer, R.P., Stassen, P., Foster, G.L., and Zachos, J.C. 2022. Surface ocean warming and acidification driven by rapid carbon release precedes Paleocene-Eocene Thermal Maximum: Science Advances, v. 8, article eabg1025, http://doi:10.1126/sciadv.abg1025.

Batten, D.J. 1985. Coccolith moulds in sedimentary organic matter and their use in palynofacies analysis: Journal of Micropalaeontology, v. 4, p. 111–116, https://doi.org/10.1144/jm.4.2.111.

Bralower, T.J., Kelly, D.C., Gibbs, S., Farley, K., Eccles, L., Lindemann, T.L., and Smith, G.J. 2014. Impact of dissolution on the sedimentary record of the Paleocene–Eocene thermal maximum: Earth and Planetary Science Letters, v. 401, p. 70–82, http://dx.doi.org/10.1016/j.epsl.2014.05.055.

Bralower, T.J., Kump, L.R., Self-Trail, J.M., Robinson, M.M., Lyons, S., Babila, T., Ballaron, E., Freeman, K.H., Hajek, E., Rush, W., and Zachos J.C. 2018. Evidence for shelf acidification during the onset of the Paleocene-Eocene Thermal Maximum. Paleoceanography and Paleoclimatology, v. 33, p. 1408–1426, https://doi.org/10.1029/2018PA003382.

Bujak, J.P., and Brinkhuis, H. 1998. Global warming and dinocyst changes across the Paleocene/Eocene Epoch boundary. In: Aubry, M.-P., Lucas, S.G., & Berggren, W.A., eds. Late Paleocene–early Eocene biotic and climatic events in the marine and terrestrial records: New York, Columbia University Press, p. 277–295.

Bybell, L.M., and Gibson, T.G. 1991. Calcareous nannofossils and foraminifers from Paleocene and Eocene strata in Maryland and Virginia. In: Gibson, T.G., and Bybell, L.M., leaders, Paleocene-Eocene boundary; sedimentation in the Potomac River Valley, Virginia and Maryland, field trip guidebook: International Geological Correlation Programme Field Trip Guidebook, October 31, 1991, p. 15–19., International Geological Correlation Programme (IGCP) Project No. 308, Paleocene Eocene Boundary.

Bybell, L.M., and Gibson, T.G 1994. Paleogene stratigraphy of the Putneys Mill, New Kent County, Virginia, corehole: U.S. Geological Survey Open-file Report 94-217: 38 pp.

Crouch, E.M., Heilmann-Clausen, C., Brinkhuis, H., Morgans, H.E.G., Rogers, K.M., Egger, H., and Schmitz, B. 2001. Global dinoflagellate event associated with the late Paleocene thermal maximum: Geology, v. 29, p. 315–318, https://doi.org/10.1130/0091-7613(2001)029<0315:GDEAWT>2.0.CO;2.

Doubrawa, M., Stassen, P., Robinson, M.M., Babila, T.L., Zachos, J.C., and Speijer, R.P. 2022. Shelf ecosystems along the U.S. Atlantic Coastal Plain prior to and during the Paleocene-Eocene Thermal Maximum: Insights into the stratigraphic architecture: Paleoceanography and Paleoclimatology, v. 37, e2022PA004475, https://doi.org/10.1029/2022PA004475.

Downie, C. 1956. Microplankton from the Kimeridge Clay: Quarterly Journal of the Geological Society, London v. 112, p. 413–434, https://doi.org/10.1144/GSL.JGS.1956.112.01-04.20.

Edwards, L.E. 2012. Dinocyst taphonomy, impact craters, cyst ghosts and the Paleocene–Eocene thermal maximum (PETM): Palynology, v. 36, p. 80–95, https://doi.org/10.1080/01916122.2012.679205.

Gibbs, S.J., Bown, P.R., Sessa, J.A., Bralower, T.J., and Wilson, P.A. 2006. Nanoplankton extinction and origination across the Paleocene-Eocene Thermal Maximum: Science, v. 314, p. 1770–1773, https://doi:10.1126/science.1133902.

Gibbs, S.J., Stoll, H.M., Bown, P.R., and Bralower T.J. 2010. Ocean acidification and surface water carbonate production across the Paleocene–Eocene thermal maximum: Earth and Planetary Science Letters, v. 295, p. 583–592, https://doi.org/10.1016/j.epsl.2010.04.044.

Gibson, T.G., and Bybell, L.M. 1994. Paleogene stratigraphy of the Solomons Island, Maryland corehole: U.S. Geological Survey Open-file Report 94-708: 39 pp.

Kender, S., Bogus, K., Pedersen, G.K., Karen Dybkjær, Tamsin A. Mather, Mariani, E., Ridgwell, A., Riding, J.B., Wagner, T., Hesselbo, S.P., and Leng, M.J. 2021. Paleocene/Eocene carbon feedbacks triggered by volcanic activity: Nature Communications, v. 12, p. 5186, https://doi.org/10.1038/s41467-021-25536-0.

Kump, L.R., Bralower, T.J., and Ridgwell, A. 2009. Ocean Acidification in Deep Time: Oceanography, v. 22, p. 94–107, https://www.jstor.org/stable/10.2307/24861027.

Martini, E. 1971. Standard Tertiary and Quaternary calcareous nannoplankton zonation. In: Farinacci, A., ed. Proceedings of the Second Planktonic Conference, Roma: Rome**,** Edizioni Tecnoscienza, 2, p. 739–785.

McArthur, J.M., Algeo, T.J., van de Schootbrugge, B., Li, Q., and Howarth, R.J. 2008. Basinal restriction, black shales, Re-Os dating, and the Early Toarcian (Jurassic) oceanic anoxic event: Paleoceanography, v. 23, p. PA4217, https://doi.org/10.1029/2008PA001607.

McInerney, F.A., and Wing, S.L., 2011. The Paleocene-Eocene Thermal Maximum: A Perturbation of Carbon Cycle, Climate, and Biosphere with Implications for the Future: Annual Review of Earth and Planetary Sciences, v. 39, p. 489–516, https://doi.org/10.1146/annurev-earth-040610-133431.

O'Dea, S.A. Gibbs, S.J., Bown, P.R., Young, J.R., Poulton, A.J., Newsam, C., and Wilson P.A. 2014. Coccolithophore calcification response to past ocean acidification and climate change: Nature Communications, v. 5, p. 5363, https://doi.org/10.1038/ncomms6363.

Penman, D.E., Hönisch, B., Zeebe, R.E., Thomas, E., and Zachos, J.C. 2014. Rapid and sustained surface ocean acidification during the Paleocene-Eocene Thermal Maximum: Paleoceanography, v. 29, p. 357–369, https://doi.org/10.1002/2014PA002621.

Robinson, M.M., and Spivey, W.E., 2019. Environmental and geomorphological changes on the Eastern North American continental shelf across the Paleocene-Eocene boundary: Paleoceanography and Paleoclimatology, v. 34, p. 715–732, https://doi.org/10.1029/2018PA003357.

Schneider-Mor, A., and Bowen, G. J. 2013. Coupled and decoupled responses of continental and marine organic-sedimentary systems through the Paleocene-Eocene Thermal Maximum, New Jersey margin, USA: Paleoceanography, v. 28, p. 105–115, https://doi.org/10.1002/palo.20016.

Self-Trail, J.M. 2011. Paleogene Calcareous Nannofossils of the South Dover Bridge core, Southern Maryland (USA): Journal of Nannoplankton Research, v. 32, p. 1–28.

Self-Trail, J.M., and Seefelt, E.L. 2005. Rapid dissolution of calcareous nannofossils: A case study from freshly cored sediments of the south-eastern Atlantic Coastal Plain. Journal of Nannoplankton Research, v. 27, p. 149–158.

Self-Trail, J.M., Powars, D.S., Watkins, D.K., Wandless, G.A. 2012. Calcareous nannofossil assemblage changes across the Paleocene–Eocene Thermal Maximum: Evidence from a shelf setting: Marine Micropaleontology, v. 92–93, p. 61–80, https://doi:10.1016/j.marmicro.2012.05.003.

Slater, S.M., Bown, P., Twitchett, R.J., Danise, S., and Vajda, V. 2022. Global record of "ghost" nannofossils reveals plankton resilience to high CO_2 and warming: Science, v. 376, p. 853–856, http://doi:10.1126/science.abm7330.

Thomas, E. 1989. Development of Cenozoic deep-sea benthic foraminiferal faunas in Antarctic waters. In: Crame, J.A., ed. Origins and evolution of the Antarctic biota. London, UK: Geological Society London Special Publication, v. 47, p. pp. 283–296, https://doi.org/10.1144/GSL.SP.1989.047.01.21.

Thomas, E. 2003. Extinction and food at the seafloor: A high-resolution benthic foraminiferal record across the initial Eocene thermal maximum, Southern Ocean site 690. In: Wing, S.L., Gingerich, P.D., Schmitz, B., and Thomas, E., eds. Causes and consequences of globally warm climates in the early Paleogene: GSA Special Papers, v. 369, p. 319–332, https://doi.org/10.1130/0-8137-2369-8.319.

Thomas, E. 2007. Cenozoic mass extinctions in the deep sea: What perturbs the largest habitat on Earth? In: Monechi, S., Coccioni, R., Rampino, M.R., eds. Geological Society of America Special Paper, v. 424, p. 1–23, http://doi:10.1130/2007.2424(01).

Turner, S.K. 2018. Constraints on the onset duration of the Paleocene–Eocene Thermal Maximum: Philosophical Transactions A, v. 376, 20170082, http://dx.doi.org/10.1098/rsta.2017.0082.

Zachos, J.C., Röhl, U., Schellenberg, S.A., Sluijs, A., Hodell, D.A., Kelly, D.C., Thomas, E., Nicolo, M., Raffi, I., Lourens, L.J., McCarren, H., Kroon, D. 2005. Rapid acidification of the ocean during the Paleocene-Eocene thermal maximum: Science, v. 308, p. 1611–1615, http://doi:10.1126/science.1109004.

FIGURE CAPTIONS

Figure 1. Location of the South Dover Bridge (SDB) core, Southern Maryland, USA. Modified from Self-Trail (2011).

Figure 2. Selected nannofossil imprints on organic matter. A, imprints on AOM, sample PJ-SDB13-004. B, small *Toweius*, enlarged image of A. C, small *Coccolithus*, enlarged image of A. D, indeterminate very small coccoliths, sample PJ-SDB13-002. E, indeterminate very small coccoliths, enlarged image of D. F, indeterminate very small coccoliths, sample PJ-SDB13-004. G, indeterminate coccoliths, PJ-SDB13-005. H, *Neochiastozygus* sp., sample PJ-SDB13-005. I, small *Calcidiscus*, sample PJ-SDB13-004. J, small *Toweius*, PJ-SDB13-004. K, *Discoaster multiradiatus*, sample PJ-SDB13-006. L, *Umbilicosphaera bramlettei*, sample PJ-SDB13-008. Red images are inverted. Arrows indicate nannofossil imprints.

Figure 3. Sedimentary log, carbon isotope, nannofossil imprint, nannoplankton body fossil, and palynofacies data through the PETM of SDB. Organic matter categories comprising <1% of the total count are excluded here. See Table S1 for sample details and raw data. Richness values for body fossils based on counts of 400 specimens (from Self-Trail et al., 2012). $CaCO_3$ (%) content data is from Doubrawa et al., (2022). Bulk carbon isotope data is from Self-Trail (2011).

Figure S1. Scanning electron micrographs of selected nannoplankton body fossils on rock surfaces. A, B, Side view of *Braarudosphaera* sp. or *Micrantholithus* sp., sample PJ-SDB13-003. C, *Blackites* sp., sample PJ-SDB13-004. D, E, *Coccolithus pelagicus*, sample PJ-SDB13-004. F, *Neochiastozygus dentatus*, sample PJ-SDB13-004. G, *Toweius eminens* (left), sample PJ-SDB13-004. H, I, *Toweius pertusus*, sample PJ-SDB13-004.

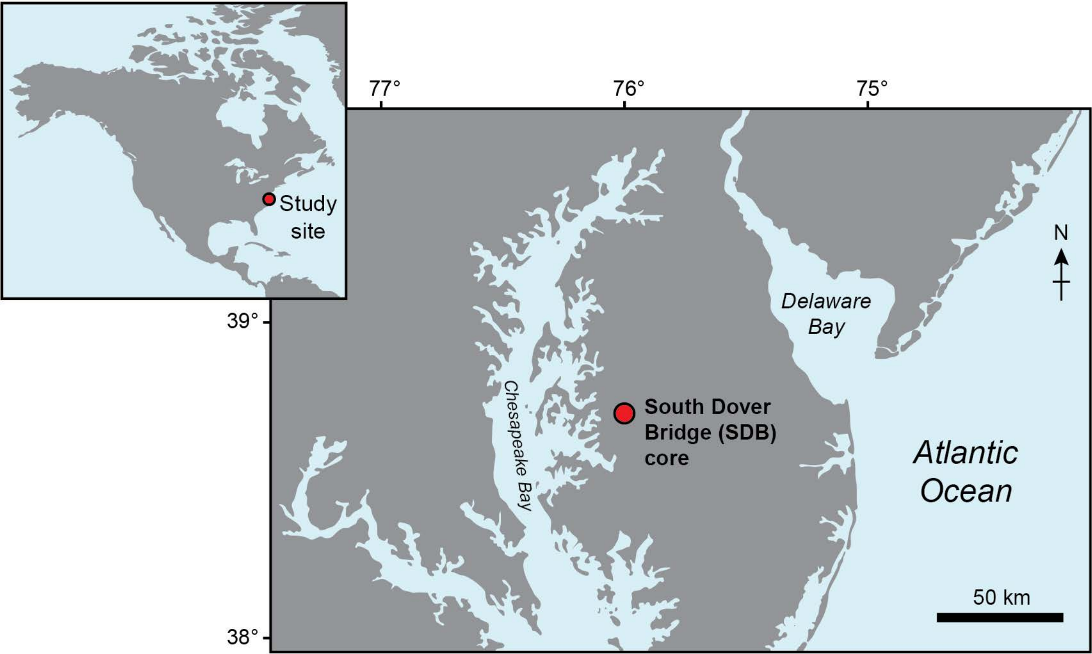
Study site
77°
76°
75°
39°
38°
N
Delaware Bay
Chesapeake Bay
South Dover Bridge (SDB) core
Atlantic Ocean
50 km

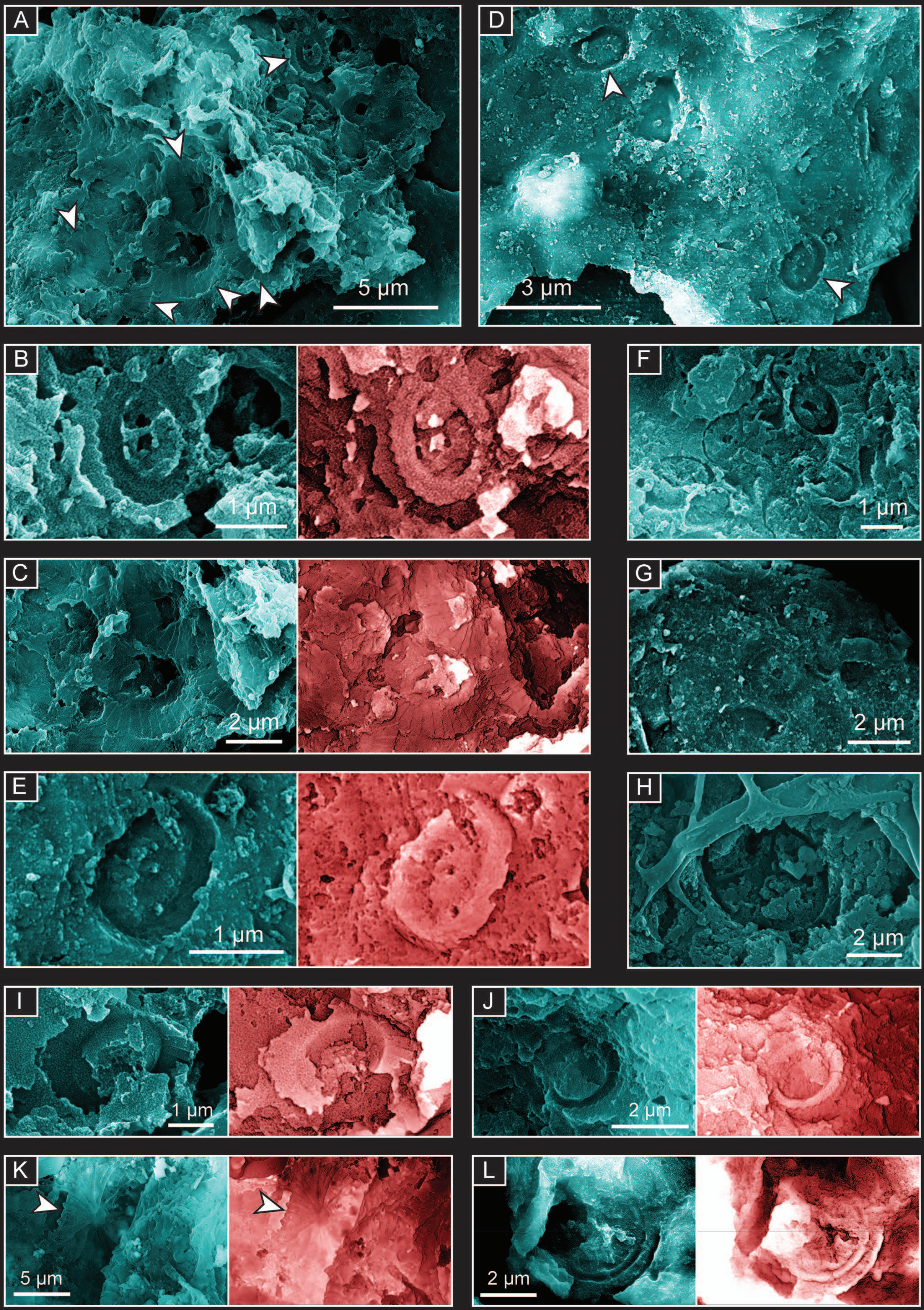
A
5 µm
D
3 µm
B
1 µm
F
1 µm
C
2 µm
G
2 µm
E
1 µm
H
2 µm
I
1 µm
J
2 µm
K
5 µm
L
2 µm

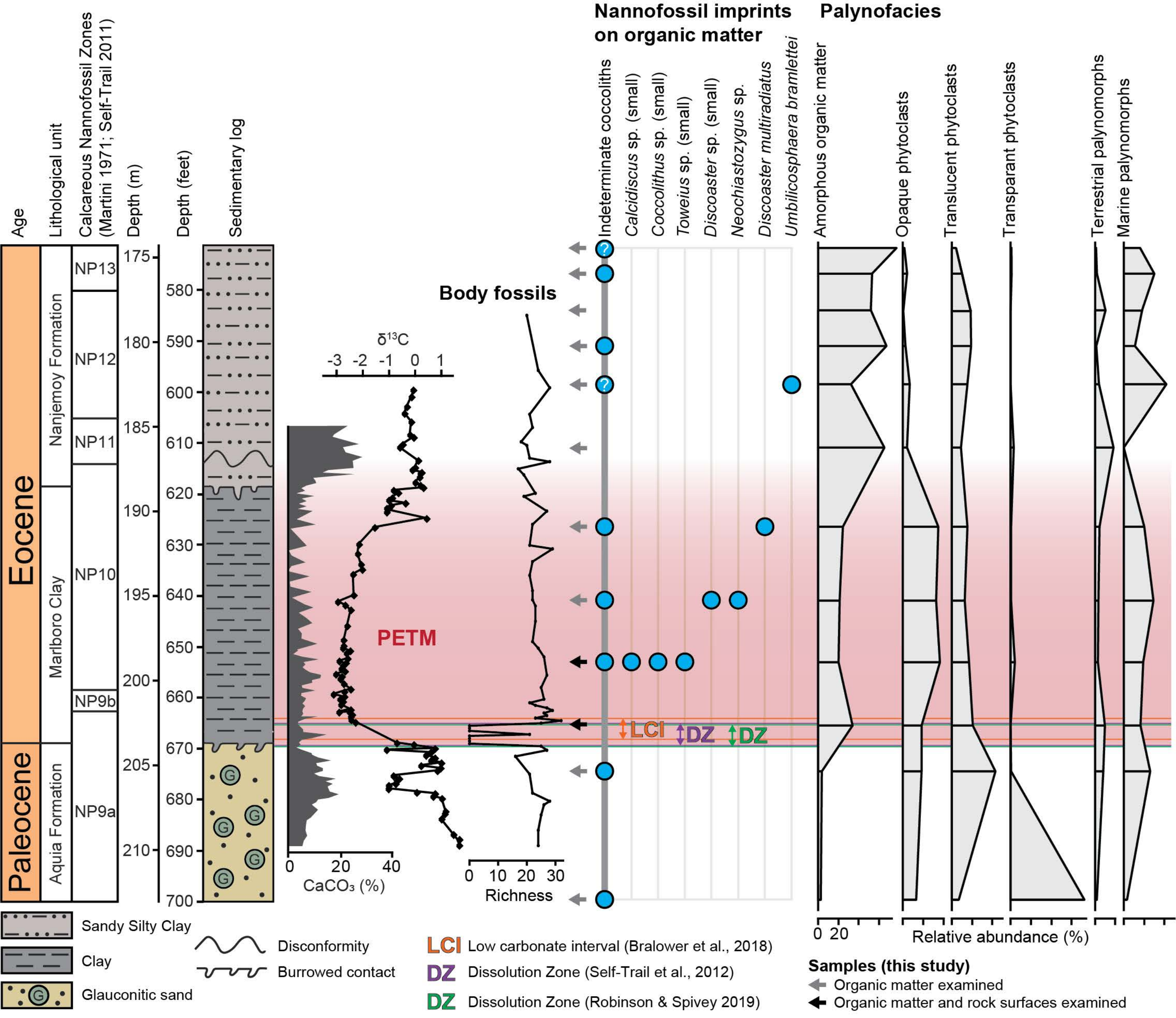

Nannofossil imprints on organic matter
Palynofacies
Age
Lithological unit
Calcareous Nannofossil Zones (Martini 1971; Self-Trail 2011)
Depth (m)
Depth (feet)
Sedimentary log
Indeterminate coccoliths
Calcidiscus sp. (small)
Coccolithus sp. (small)
Toweius sp. (small)
Discoaster sp. (small)
Neochiastozygus sp.
Discoaster multiradiatus
Umbilicosphaera bramlettei
Amorphous organic matter
Opaque phytoclasts
Translucent phytoclasts
Transparant phytoclasts
Terrestrial palynomorphs
Marine palynomorphs
Eocene
Paleocene
Nanjemoy Formation
Marlboro Clay
Aquia Formation
NP13
NP12
NP11
NP10
NP9b
NP9a
Body fossils
δ13C
PETM
LCI
DZ
DZ
CaCO3 (%)
Richness
Relative abundance (%)
Sandy Silty Clay
Clay
Glauconitic sand
Disconformity
Burrowed contact
LCI Low carbonate interval (Bralower et al., 2018)
DZ Dissolution Zone (Self-Trail et al., 2012)
DZ Dissolution Zone (Robinson & Spivey 2019)
Samples (this study)
Organic matter examined
Organic matter and rock surfaces examined

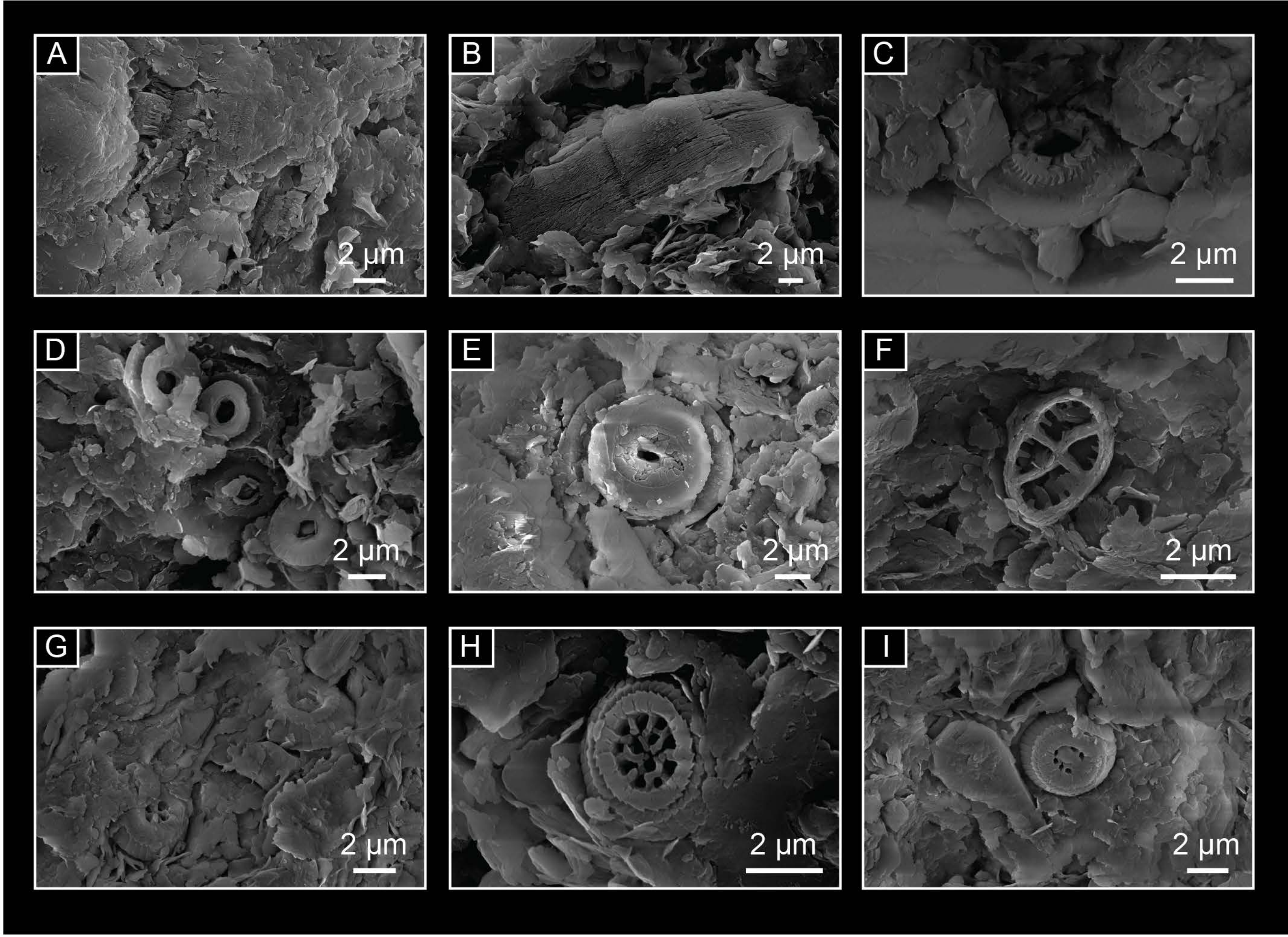

Figure S1. Scanning electron micrographs of selected nannoplankton body fossils on rock surfaces. A, B, Side view of *Braarudosphaera* sp. or *Micrantholithus* sp., sample PJ-SDB13-003. C, *Blackites* sp., sample PJ-SDB13-004. D, E, *Coccolithus pelagicus*, sample PJ-SDB13-004. F, *Neochiastozygus dentatus*, sample PJ-SDB13-004. G, *Toweius eminens* (left), sample PJ-SDB13-004. H, I, *Toweius pertusus*, sample PJ-SDB13-004.